

A MAXIMUM NOISE FRACTION TRANSFORM BASED ON A SENSOR NOISE MODEL FOR HYPERSPECTRAL DATA

Naoto Yokoya¹ and Akira Iwasaki²

¹Graduate Student, Department of Aeronautics and Astronautics, The University of Tokyo,
4-6-1 Komaba, Meguro-ku, Tokyo 153-8904, Japan; Tel: + 81-3-5452-5319;
E-mail: yokoya@sal.rcast.u-tokyo.ac.jp

²Professor, Research Center for Advanced Science and Technology, The University of Tokyo,
4-6-1 Komaba, Meguro-ku, Tokyo 153-8904, Japan; Tel: + 81-3-5452-5285;
Email: aiwasaki@sal.rcast.u-tokyo.ac.jp

KEY WORDS: feature extraction, MNF transform, noise estimation, hyperspectral data, spectral distortion

ABSTRACT: The maximum noise fraction (MNF) transform, which produces the improved order of components by signal to noise ratio (SNR), has been commonly used for spectral feature extraction from hyperspectral remote sensing data before image classification. When hyperspectral data contains a spectral distortion, also known as a “smile” property, the first component of the MNF, which should have high image quality, suffers from noisy brightness gradient pattern which thus reduces classification accuracy. This is probably because the classic noise estimation of the MNF is different from the real noise model. The noise estimation is the most important procedure because the noise covariance matrix determines the characteristics of the MNF transform. An improved noise estimation method from a single image based on a noise model of a charge coupled device (CCD) sensor is introduced to enhance the feature extraction performance of the MNF. This method is applied to both airborne and spaceborne hyperspectral data, acquired from the airborne visible infrared/imaging spectrometer (AVIRIS) and the EO-1/Hyperion, respectively. The experiment for the Hyperion data demonstrates that the proposed MNF is resistant to the spectral distortion of hyperspectral data. Furthermore, the image classification experiment for the AVIRIS Indian pines data using the MNF as a preprocessing step to extract spectral features shows that the proposed method extracts higher SNR components in lower MNF components than the existing feature extraction methods.

1. INTRODUCTION

Hyperspectral data contains hundreds of spectral bands collecting spectrograms continuously with a pushbroom imaging system. At each pixel, a continuous spectral profile can be obtained, which enables discrimination among land-cover classes that are spectrally similar (Kruse *et al.*, 2003). Before classifying these ground surface objects, spectral feature extraction is commonly performed, such as the principal component analysis (PCA) and the maximum noise fraction (MNF) transform. PCA generates linear combinations of hyperspectral pixel radiance which are mutually uncorrelated and have maximum variance. Since hyperspectral data always contains noise, PCA extracts noisy images in low order components due to no consideration of image noise. MNF transform was developed to produce new components ordered by image quality maximizing the signal to noise ratio (SNR) rather than maximizing variance (Green *et al.*, 1988). It has been commonly used for spectral dimensionality reduction of hyperspectral data (Underwood *et al.*, 2003; Mundt *et al.*, 2005).

Hyperspectral data contains spectral distortion also known as a “smile” property. Smile property is a wavelength shift in spectral domain expressed as a function of the cross-track pixel number. Past researches showed that MNF transform suffers from smile property (Goodenough *et al.*,

2003; Dadon *et al.*, 2010). When MNF transform is applied to hyperspectral data with smile distortion, brightness gradients in the cross-track direction appear in the first component. These artifacts never represent spectral features of ground surface objects and thus degrade classification results. Enhancement of smile distortion as a brightness gradient in MNF occurs because noise estimation in MNF is different from the real noise model. In this work, we propose a new MNF transform improving noise estimation based on a sensor noise model. Resistance to smile property and performance of spectral dimensionality reduction before classification are evaluated applying the proposed method to airborne and spaceborne hyperspectral data.

2. MNF BASED ON A SENSOR NOISE MODEL

2.1 Classic MNF

A hyperspectral profile \mathbf{x} at each pixel can be expressed as $\mathbf{x} = \mathbf{s} + \mathbf{n}$, where \mathbf{s} and \mathbf{n} represent the signal and noise part of data, respectively. When both components are assumed to be normally distributed with respective covariance matrices Σ_s and Σ_n , to have zero mean, and to be uncorrelated, the covariance of observed data is given by $\Sigma = \Sigma_s + \Sigma_n$. Let us seek a linear combination $\mathbf{y} = \mathbf{A}'\mathbf{x}$ to maximize the SNR. \mathbf{A} is the MNF transform matrix defined by $\mathbf{A} = (\mathbf{a}_1, \mathbf{a}_2 \dots \mathbf{a}_n)$, where \mathbf{a}_i is the i th order transform vector. The SNR of the new component is given by

$$SNR = \frac{\mathbf{a}' \Sigma_x \mathbf{a}}{\mathbf{a}' \Sigma_n \mathbf{a}} - 1.$$

Setting its vector derivative with respect to \mathbf{a} equal to zero, we get the generalized eigenvalue problem given by

$$\Sigma_n \mathbf{a} = \lambda \Sigma_x \mathbf{a}.$$

Noise estimation is the most important procedure that determines the performance of MNF transform. The classic MNF transform for remote sensing data analysis supposes that an observed target at a pixel is almost the same at neighboring pixels, and thus estimates noise as follows:

$$\mathbf{n}_{i,j} = \mathbf{x}_{i,j} - \frac{1}{2}(\mathbf{x}_{i+1,j} + \mathbf{x}_{i,j+1}).$$

Here, i and j denote the cross-track and along-track positions, respectively. Many past studies show the effectiveness of this classic MNF transform for spectral dimensionality reduction of hyperspectral data (Underwood *et al.*, 2003; Mundt *et al.*, 2005). However, as mentioned in the introduction, when there is smile distortion at some level, brightness smile gradient appears in the first MNF component, as shown in the lower images of Figure 2. This phenomenon degrades the performance of MNF transform for feature extraction and reduces classification accuracy.

2.2 Noise Estimation Based on a Sensor Noise Model

We adopt a noise estimation method based on a sensor noise model that estimates the noise dependent on radiance (Liu *et al.*, 2008). A charge coupled device (CCD) imaging sensor is commonly used for the two-dimensional detector array of satellite hyperspectral sensors. The CCD imaging sensor produces five primary noise sources, namely, fixed pattern noise, dark current noise, shot noise, amplifier noise and quantization noise (Healy & Kondepudy, 1994). They can be classified into two noises, dependent and independent on radiance. We focus on estimating the noise dependent on radiance.

First, we estimate the noise level function (NLF), which is a continuous function describing the noise level as a function of image brightness. The NLF f_{NL} is defined as the standard deviation with respect to image intensity. The problem is how to measure the NLF only from observed images. We estimate the NLFs in all bands by the block based noise level estimation as follows. In all bands, each image component is divided into blocks of size $N \times N$. Then, for all blocks, the mean (μ) and standard deviation (σ) are calculated. Finally, the lower envelope, which is the calculated

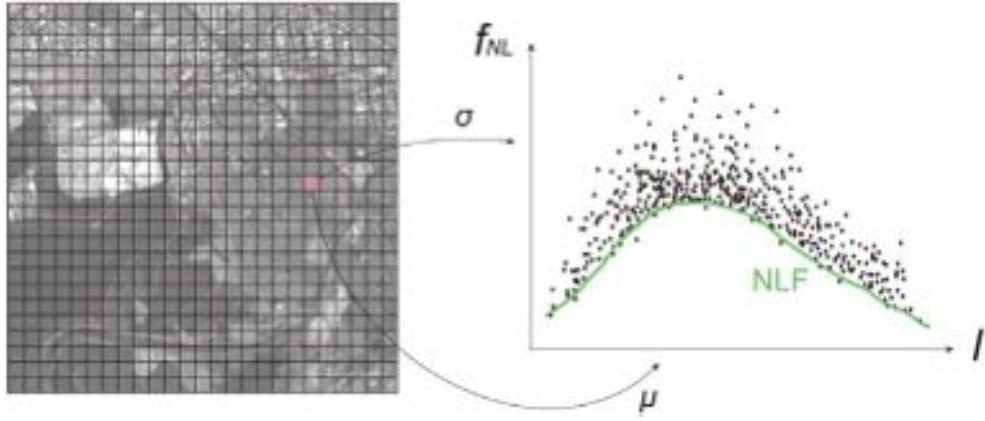


Figure 1. Noise level function.

NLF estimation, is fit to the sample set (μ, σ) , as shown in Figure 1. We adopt the 95 percentile method, which approximates the lower envelope as the value over which 95 percent of observations can be found. After the NLF estimation, the signal part $s(\mathbf{z})$ of the original value $x(\mathbf{z})$ is estimated by bilateral filtering (Tomasi & Manduchi, 1998) with the consideration of NLF, where \mathbf{z} is a position (i, j) for a certain band. Bilateral filtering is given by

$$s(\mathbf{z}) = k(\mathbf{z})^{-1} \int_{-\infty}^{\infty} \int_{-\infty}^{\infty} x(\mathbf{z}) g(\xi, \mathbf{z}) p(x(\xi), x(\mathbf{z})) d\xi,$$

with the normalization

$$k(\mathbf{z}) = \int_{-\infty}^{\infty} \int_{-\infty}^{\infty} g(\xi, \mathbf{z}) p(x(\xi), x(\mathbf{z})) d\xi.$$

Here, $g(\xi, \mathbf{z})$ and $p(x(\xi), x(\mathbf{z}))$ denote the geometric closeness and the photometric similarity, respectively, between the neighborhood center \mathbf{z} and a nearby point ξ . For the closeness function $g(\xi, \mathbf{z})$ and the similarity function $p(x(\xi), x(\mathbf{z}))$, we use Gaussian functions defined as follows:

$$g(\xi, \mathbf{z}) = \exp\left(-\frac{1}{2} \left(\frac{d(\xi, \mathbf{z})}{\sigma_g}\right)^2\right), \quad p(\xi, \mathbf{z}) = \exp\left(-\frac{1}{2} \left(\frac{\delta(x(\xi), x(\mathbf{z}))}{\sigma_p}\right)^2\right),$$

where $d(\xi, \mathbf{z}) = \|\xi - \mathbf{z}\|$, $\delta(x(\xi), x(\mathbf{z})) = \|x(\xi) - x(\mathbf{z})\|$, and σ_g and σ_p denote the geometric and photometric spread parameters, respectively. In this work, we set σ_g as 1, and σ_p as an output of the NLF. Finally, the noise part $n(\mathbf{z})$ of the original value $x(\mathbf{z})$ is given by $n(\mathbf{z}) = x(\mathbf{z}) - s(\mathbf{z})$.

3. RESULTS AND DISCUSSIONS

In this section, the proposed MNF transform is evaluated by the following two points, the resistance to smile property and the spectral dimensionality reduction performance before classification.

3.1 Resistance for Smile Property

The classic and proposed MNF transforms were applied to the EO-1/Hyperion/VNIR band 8-57 taken over various eight scenes. Comparisons of the MNF 1st component between the classic and proposed MNF transforms are shown in Figure 2. In the classic MNF, brightness gradient in the cross-track direction caused by smile property appeared in the first component for all imageries. On the other hand, this artifact did not appear in the proposed MNF. This means that the new MNF transform is little affected by smile property, which contributes to improved classification mapping for hyperspectral data. Originally, the information of smile distortion should be small in the entire hyperspectral data information. Therefore, the new MNF shows better performance than the classic counterpart as the feature extraction methods which should produce higher SNR images in lower order components.

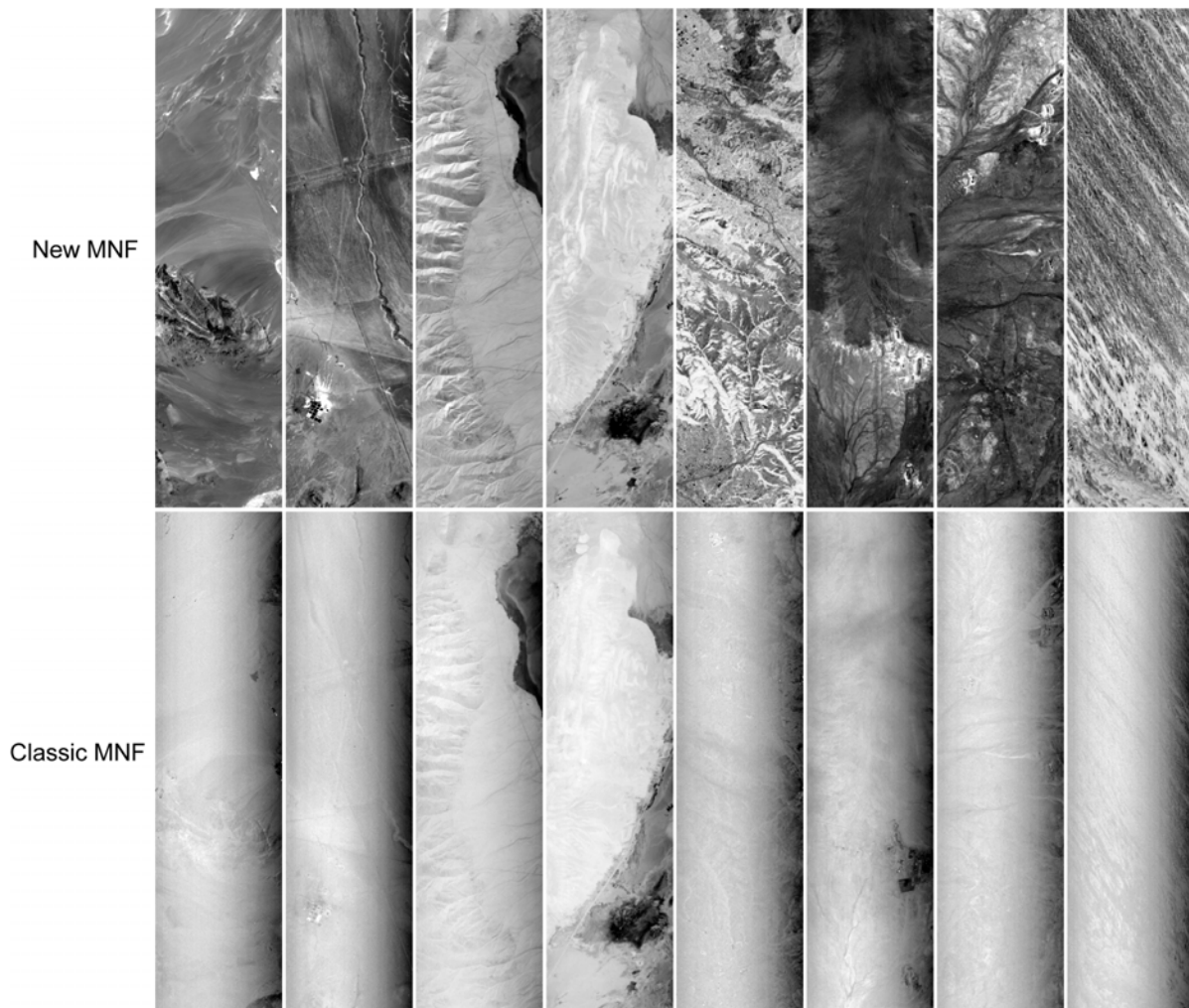


Figure 2. Comparison of the MNF 1st component between the classic (lower images) and proposed (upper images) MNF transforms

3.2 Spectral Dimensionality Reduction

The spectral dimensionality reduction performance of the proposed method was examined by hyperspectral data classification experiment comparing the method with PCA, classic MNF, and spectral MNF. Spectral MNF (Liu *et al.*, 2009) is a MNF transform that improves noise estimation using a neighboring band image correlation for a certain band. We used the AVIRIS data taken over Indian pines (USA) in 1992. This data set was chosen because its ground truth is available. The data consists of 145x145 pixels with 220 bands. Its true color image and the class map are shown in Figure 3. First, the spectral dimensionality of the data was reduced by feature extraction. Then, this image was classified using spectral angle mapper (SAM) commonly used as classifier. All ground truth samples were used for test data and 20% of the data were randomly selected for training data. Average spectra of training data were set as the reference spectra. This experiment was iterated 20 times. Figure 4 shows the comparison between four feature extraction methods regarding the relationship between classification accuracies and feature component numbers used for classification. Mapping results, with feature component number b set to 4, 10 and 20, are shown in Figure 5. Classification accuracy of the proposed new MNF outperforms the others when feature component number is less than twelve. This means that this method extracts higher quality features of hyperspectral data in lower order components than the others. When feature component number is over twelve, classification accuracy remains at the same level and is reversed by the classic and spectral MNFs. This is probably because noisy images also appear in lower order components. In the noise estimation of the new MNF, there are some parameters, which affect classification accuracy. Determination of these parameters is a future task.

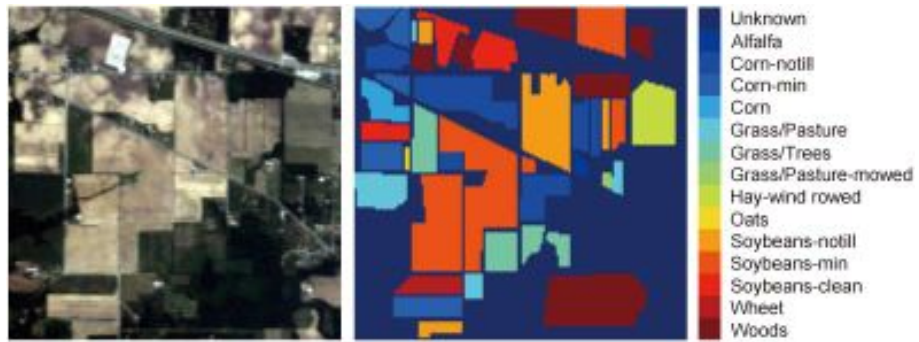


Figure 3. The true color and class map for the AVIRIS Indian Pine data.

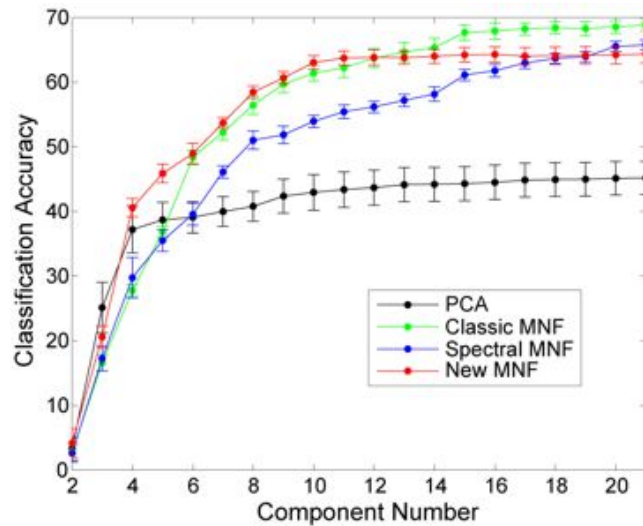


Figure 4. Comparison of relationship between classification accuracies and feature component numbers used for classification for different four feature extraction methods.

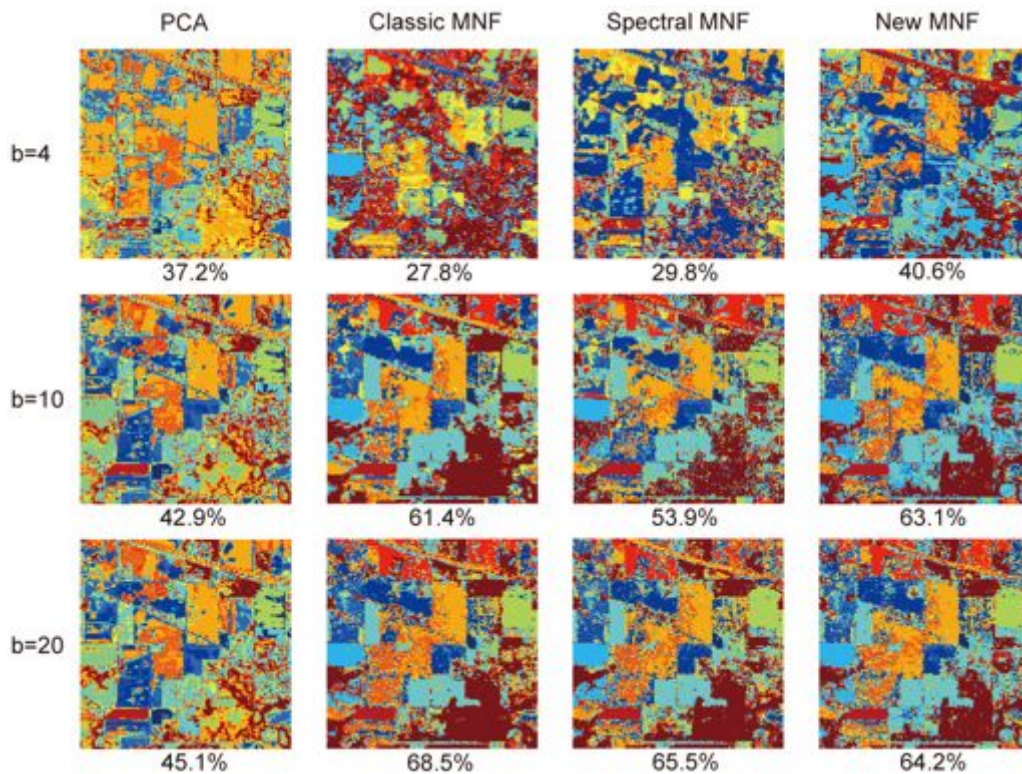


Figure 5. Classification mapping results. Percentage values below images are classification accuracies.

4. CONCLUSION

In this work, we proposed the new MNF transform based on the sensor noise model. Noise estimation procedure was improved by estimating image noise dependent on measured radiance using the NLF. The effectiveness of this method was proved from two points of view. One is the resistance for smile property, which makes the brightness gradient found in the first component of the classic MNF. When applying the proposed method to the EO-1/Hyperion data, the first component of the new MNF is not affected by smile property. The other is the performance of spectral dimensionality reduction as a preprocessing of hyperspectral classification mapping. From the classification experiment using the AVIRIS data, it turned out that the proposed method extracts higher SNR components in lower MNF components than the existing feature extraction methods.

REFERENCES

Dadon, A., Ben-Dor, E., and Karnieli, A., 2010. Use of derivative calculations and minimum noise fraction transform for detecting and correcting the spectral curvature effect (smile) in Hyperion images. *IEEE Trans. Geosci. Remote Sens.*, 48(6), pp. 2603-2612.

Goodenough, D. G., Dyk, A., Niemann, K. O., Pearlman, J. S., Chen, H., Han, T., Murdoch, M., and West, C., 2003. Processing Hyperion and ALI for forest classification. *IEEE Trans. Geosci. Remote Sens.*, 41(6), pp. 1321-1331.

Green, A. A., Berman, M., Switzer, P., and Craig, M. D., 1988. A transformation for ordering multispectral data in terms of image quality with implications for noise removal. *IEEE Trans. Geosci. Remote Sens.*, 26(1), pp. 65-74.

Kruse, F. A., Boardman, J. W., and Huntington, J. F., 2003. Comparison of airborne hyperspectral data and EO-1 Hyperion for mineral mapping. *IEEE Trans. Geosci. Remote Sens.*, 41(6), pp. 1388-1400.

Liu, C., Szeliski, R., Kang, S. B., Zitnick, C. L., and Freeman, W. T., 2008. Automatic estimation and removal of noise from a single image. *IEEE Trans. Pattern Anal. Mach. Intell.*, 30(2), pp. 299-314.

Liu, X., Zhang, B., Gao, L., and Chen, D., 2009. A maximum noise fraction transform with improved noise estimation for hyperspectral images. *Sci. China Ser. F-Inf. Sci.* 52, pp. 1578-1587.

Mundt, J. T., Glenn, N. F., Weber, K. T., Prather, T. S., Lass, L. W., and Pettingill, J., 2005. Discrimination of hoary cress and determination of its detection limits via hyperspectral image processing and accuracy assessment techniques. *Remote Sens. Environ.*, 96, pp. 509-517.

Tomasi, C. and Manduchi, R., 1998. Bilateral filtering for gray and color images. *Proc. IEEE Int'l Conf. Computer Vision*, pp. 839-846.

Underwood, E., Ustin, S., and DiPietro, D., 2003. Mapping nonnative plants using hyperspectral imagery. *Remote Sens. Environ.*, 86, pp. 150-161.